

Beyond Nyquist in Frequency Response Function Identification Applied to Slow-Sampled Systems

Van Haren, Max; Mirkin, Leonid; Blanken, Lennart; Oomen, Tom

DOI

[10.1109/LCSYS.2023.3284344](https://doi.org/10.1109/LCSYS.2023.3284344)

Publication date

2023

Document Version

Final published version

Published in

IEEE Control Systems Letters

Citation (APA)

Van Haren, M., Mirkin, L., Blanken, L., & Oomen, T. (2023). Beyond Nyquist in Frequency Response Function Identification: Applied to Slow-Sampled Systems. *IEEE Control Systems Letters*, 7, 2131-2136. <https://doi.org/10.1109/LCSYS.2023.3284344>

Important note

To cite this publication, please use the final published version (if applicable).
Please check the document version above.

Copyright

Other than for strictly personal use, it is not permitted to download, forward or distribute the text or part of it, without the consent of the author(s) and/or copyright holder(s), unless the work is under an open content license such as Creative Commons.

Takedown policy

Please contact us and provide details if you believe this document breaches copyrights.
We will remove access to the work immediately and investigate your claim.

Beyond Nyquist in Frequency Response Function Identification: Applied to Slow-Sampled Systems

Max van Haren¹, Leonid Mirkin², *Member, IEEE*, Lennart Blanken³,
and Tom Oomen⁴, *Senior Member, IEEE*

Abstract—Fast-sampled models are essential for control design, e.g., to address intersample behavior. The aim of this letter is to develop a non-parametric identification technique for fast-sampled models of systems that have relevant dynamics and actuation above the Nyquist frequency of the sensor, such as vision-in-the-loop systems. The developed method assumes smoothness of the frequency response function, which allows to disentangle aliased components through local models over multiple frequency bands. The method identifies fast-sampled models of slowly-sampled systems accurately in a single identification experiment. Finally, an experimental example demonstrates the effectiveness of the technique.

Index Terms—Frequency response function, sampled-data systems, system identification.

I. INTRODUCTION

SYSTEMS that have actuation and dynamics above the Nyquist frequency of the sensor, known as slow-sampled systems, are becoming increasingly common in for example vision-in-the-loop systems. As a consequence of the Nyquist-Shannon sampling theorem [1], slow-sampled systems are

Manuscript received 17 March 2023; revised 17 May 2023; accepted 4 June 2023. Date of publication 8 June 2023; date of current version 27 June 2023. This work was supported in part by the Research Programme VIDI, which is (partly) financed by the Netherlands Organisation for Scientific Research (NWO) under Project 15698; in part by the ECSEL Joint Undertaking under Grant 101007311 (IMOCO4.E), that receives support from the European Union Horizon 2020 Research and Innovation Programme; and in part by the Israel Science Foundation (grant no. 3177/21). Recommended by Senior Editor C. Manzie. (Corresponding author: Max van Haren.)

Max van Haren is with the Control Systems Technology Section, Department of Mechanical Engineering, Eindhoven University of Technology, 5612 AE Eindhoven, The Netherlands (e-mail: m.j.v.haren@tue.nl).

Leonid Mirkin is with the Faculty of Mechanical Engineering, Technion—IIT, Haifa 3200003, Israel.

Lennart Blanken is with the Control Systems Technology Section, Department of Mechanical Engineering, Eindhoven University of Technology, 5612 AE Eindhoven, The Netherlands, and also with Sioux Technologies, 5633 AA Eindhoven, The Netherlands.

Tom Oomen is with the Control Systems Technology Section, Department of Mechanical Engineering, Eindhoven University of Technology, 5612 AE Eindhoven, The Netherlands, and also with the Delft Center for Systems and Control, Delft University of Technology, 2628 CD Delft, The Netherlands.

Digital Object Identifier 10.1109/LCSYS.2023.3284344

typically identified up to the Nyquist frequency of the slow-sampled sensor. In sharp contrast, fast-sampled models of systems are typically required for control design and performance evaluation, e.g., for the use in evaluating intersample performance [2].

Non-parametric frequency-domain representations are often used for performance evaluation and controller design of linear time-invariant (LTI) systems. An example is manual loop-shaping [3] and parametric system identification [4]. A common method for frequency-domain representation is through Frequency Response Functions (FRFs). FRFs can directly be identified from input-output data and are fast, accurate, and inexpensive to obtain [5], [6]. Finally, FRFs allow for direct evaluation of stability, performance, and robustness [7].

The identification of fast-sampled models for slow-sampled systems is challenging, since the maximum achievable identification frequency of traditional FRF identification for LTI systems is limited by the Nyquist frequency of the slow-sampled sensor. The key reason is that fast-sampled outputs are aliased when sampled by a slow-sensor, resulting in indistinguishable contributions in the output, and hence, a fast-sampled model cannot be uniquely recovered [8]. As a result, techniques for identifying fast-sampled models for slow-sampled systems, that are required for control design and performance evaluation, are necessary.

Important developments have been made in identification techniques for slow-sampled systems, primarily in continuous-time and multirate parametric system identification. First, continuous-time system identification aims to identify a continuous-time parametric model using input-output data, as outlined in [9]. Typically, these methods require intersample assumptions on the input signal, e.g., zero-order hold or bandlimited signals [10]. Second, parametric identification of slow-sampled systems are developed and include methods for impulse response [11] and output-error [12] model estimation. Lifting techniques, such as using subspace [13], frequency-domain [14] or hierarchical identification techniques [15], are also developed. These methods focus on parametric identification, require intersample assumptions on the input signal and do not exploit fast-sampled inputs, and consequently, do not disentangle aliased components.

Although methods for identification beyond the Nyquist frequency of slow-sampled systems have been developed, an efficient and systematic methodology for single-experiment FRF identification of fast-sampled models, that disentangles aliased components with arbitrary input signals, is currently lacking. In this letter, slow-sampled systems are identified with excitation signals that cover the full frequency spectrum, where aliased components are disentangled from each other through exploiting the assumption of smooth behavior in the frequency response of a system. Generally, this assumption is at the basis of modern FRF identification, as seen in techniques for LTI single-rate systems, such as Local Polynomial Modeling (LPM) [5] or local rational modeling [16]. In fact, LPM for LTI single-rate systems is recovered as a special case of the developed framework. The key contributions of this letter include the following.

- C1 Identification of non-parametric fast-sampled models for slow-sampled systems, by exciting the full frequency spectrum and aliased components are disentangled from each other by assuming smooth behavior in the frequency domain (Section IV).
- C2 Validation of the framework for identification of slow-sampled systems in an experimental setup (Section V).

Notation: Fast-sampled signals are denoted by subscript h and slow-sampled signals by subscript l . The N -points and M -points Discrete Fourier Transform (DFT) for finite-time fast-sampled and slow-sampled signals are given by

$$\begin{aligned} X_h(k) &= \sum_{n=0}^{N-1} x_h(n) e^{-j\Omega_k n T_{s,h}}, \\ X_l(k) &= \sum_{m=0}^{M-1} x_l(m) e^{-j\Omega_k m T_{s,l}} \\ &= \sum_{n=0}^{M-1} x_h(nF) e^{-j\Omega_k n T_{s,l}}, \end{aligned} \quad (1)$$

with sampling times T_h and T_l , discrete-time indices for fast-sampled signals $n \in \mathbb{Z}_{[0, N-1]}$ and slow-sampled signals $m \in \mathbb{Z}_{[0, M-1]}$ with integers \mathbb{Z} and N, M the amount of data points of the fast-sampled and slow-sampled signals and frequency bin $k \in \mathbb{Z}$, that relates to the frequency grid

$$\Omega_k = \frac{2\pi k}{NT_h} = \frac{2\pi k}{MT_l}. \quad (2)$$

The sampling times of the slow-sampled and fast-sampled signals relate as $T_l = FT_h$, with downsampling factor $F \in \mathbb{Z}_{>0}$. Hence, the signal lengths relate as $N = FM$. The complex conjugate of A is denoted as \bar{A} and the complex conjugate transpose as A^H . The complement of sets is given by $A \setminus B$. The expected value of a random variable X is given by $\mathbb{E}\{X\}$.

II. PROBLEM FORMULATION

In this section, the problem that is considered in this letter is presented. First, the identification setting is presented. Finally, the problem addressed in this letter is defined.

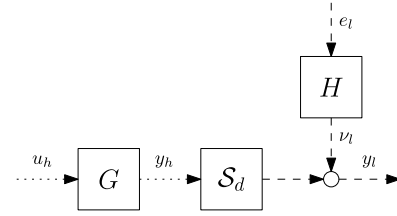


Fig. 1. Identification setting considered for slow-sampled systems.

A. Identification Setting

The goal is to identify a fast-sampled non-parametric model G with sampling rate $f_h = \frac{1}{T_h}$, using the slow-sampled output y_l with sampling rate $f_l = \frac{1}{T_l} = \frac{1}{F}f_h$, where the open-loop control structure considered is visualized in Fig. 1.

The system G and the noise model H are LTI Single-Input Single-Output (SISO) systems. The input-output behavior of LTI SISO systems in the frequency domain is given by

$$Y_h(k) = G(\Omega_k)U_h(k) + T_G(\Omega_k), \quad (3)$$

with system transient term $T_G(\Omega_k)$, that appears since the signals are finite length [5]. This reveals that a single frequency of Y_l is influenced by a single frequency of U_h , also called the frequency-separation principle. The measured slow-sampled output is a downsampled version of the fast-sampled output as shown in Fig. 1, i.e.,

$$Y_l(k) = S_d Y_h(k) + V_l(k), \quad (4)$$

with noise $V_l(k) = H(\Omega_k)E(k)$, where $E(k)$ is filtered zero-mean white noise, and is assumed to be independent and identically distributed. The transient of the noise system H is typically neglected [5, Sec. 6.7.3.4]. In time-domain, the downsampling operation in (4) equates to $S_d y_h(n) = y_h(nF)$. By applying the downsampling operation in (4), the DFT of the slow-sampled output is given by [17]

$$Y_l(k) = \frac{1}{F} \sum_{f=0}^{F-1} Y_h(k + Mf) + V_l(k). \quad (5)$$

By substituting the input-output behavior of the fast-sampled system $G(\Omega_k)$ in (3), the slow-sampled output is given by

$$Y_l(k) = \frac{1}{F} \sum_{f=0}^{F-1} (G(\Omega_{k+Mf})U_h(k + Mf) + T_G(\Omega_{k+Mf})) + V_l(k). \quad (6)$$

B. Problem Definition and Approach

The DFT Y_l in (6), for a single frequency bin k , is influenced by F frequencies of G and U_h . This is caused by aliasing due to the downsampling operation. Hence, the fast-rate system $G(\Omega_k)$ can in general not be uniquely identified with the slow-sampled output Y_l for arbitrary inputs U_h .

The problem considered in this letter is as follows. Given fast-sampled input data u_h and slow-sampled output signal y_l with DFTs U_h and Y_l shown in (4), identify a fast-sampled model of $G(\Omega_k)$ in the frequency-domain for bins $k \in \mathbb{Z}_{[0, N-1]}$, i.e., up until the fast-sampled sampling frequency f_h , for the identification setup seen in Fig. 1. The approach is developed in two steps.

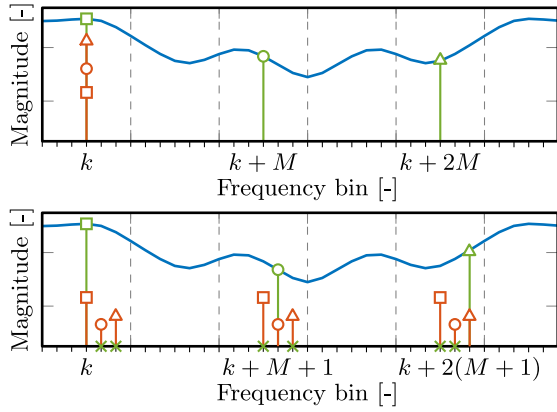


Fig. 2. Illustration of problem (top) and intuitive idea (bottom) for identifying a fast-sampled model of $G(\Omega_k)$ (—) with slow-sampled output Y_l . The Nyquist frequency and multiples when sampling the output a factor $F = 3$ slower is shown as (---). Top: Non-zero input $U(k+iM) \forall i \in \{0, 1, 2\}$ and associated gain $|G(\Omega_{k+iM})|$ (—) show that the slow-sampled output $Y_l(k)$ (—) is a summation as in (7), resulting in $F = 3$ unknowns, but only 1 equation. Bottom: Non-zero input $U(k+i(M+1)) \forall i \in \{0, 1, 2\}$ and associated gain $|G(\Omega_{k+i(M+1)})|$ (—) result in a single contribution of the summation in (7) influencing $Y_l(k+i)$ (—) by deliberately not exciting specific bins (\times). Hence, the fast-sampled system $G(\Omega_{k+i(M+1)})$ can be uniquely recovered at frequency bins $k+i(M+1)$.

- 1) Development of an intuitive idea in Section III for identifying slow-sampled systems using a dedicated input signal for a sparse frequency grid.
- 2) Development of the full approach in Section IV using arbitrary input signals and full frequency grids, leading to contribution C1.

III. INTUITIVE IDEA: IDENTIFICATION WITH SPARSE FREQUENCY SPECTRUM

The first step in Section II-B is developed, where aliasing is precisely traced for each input signal such that the slow-sampled output $Y_l(k)$ is only influenced by a single fast-sampled input $U_h(k)$. This step is intended for conveying the intuitive idea, leading to the full approach, i.e., the second step in Section II-B, in Section IV.

The transient contribution $T_G = 0$ in this section, meaning that the transient is neglected to facilitate the development of the intuitive idea, in that case (6) is equal to

$$Y_l(k) = \frac{1}{F} \sum_{f=0}^{F-1} (G(\Omega_{k+Mf})U_h(k+Mf)) + V_l(k), \quad (7)$$

showing that the slow-sampled output is a summation of the baseband response for $f = 0$, and aliased components for $f \in \mathbb{Z}_{[1, F-1]}$. Due to the summation of the baseband and aliased contributions, the fast-sampled system can in general not be uniquely recovered from slow-sampled output Y_l . An example is seen in the top of Fig. 2.

The key idea is that by designing the input signal U_h such that the output at frequency bin k is only influenced by a single contribution of the summation $G(\Omega_{k+Mf})U_h(k+Mf)$ in (7), the fast-sampled system can be recovered for a subset of all

frequency bins. This means that input signals of the form

$$\begin{cases} U_h(k+Mf) \neq 0, f = i, i \in \mathbb{Z}_{[0, F-1]}, \\ U_h(k+Mf) = 0, \mathbb{Z}_{[0, F-1]} \setminus i, \end{cases} \quad (8)$$

result in the input-output behavior

$$Y_l(k) = \frac{1}{F} G(\Omega_{k+iM})U_h(k+iM) + V_l(k), \quad (9)$$

which shows that the summation disappears, and hence, the fast-sampled system G can be uniquely recovered for the frequency bins $k+iM$. The sparse set of excited frequencies is from now on denoted by \mathcal{S} , i.e., the signal in (8) can be represented by $U_h(k) \neq 0 \forall k \in \mathcal{S}$ and $U_h(k) = 0 \forall k \notin \mathcal{S}$. The general concept of identifying slow-sampled systems with sparse multisines is shown in the bottom of Fig. 2. By noting that $Y_l(k) = Y_l(k+iM)$, $V_l(k) = V_l(k+iM) \forall i \in \mathbb{Z}$, due to the M -periodicity of the DFT, (9) is rewritten as

$$Y_l(k+iM) = \frac{1}{F} G(\Omega_{k+iM})U_h(k+iM) + V_l(k+iM), \quad \forall i \in \mathbb{Z}_{[0, F-1]}, (k+iM) \in \mathcal{S}. \quad (10)$$

An estimate of the system G is given by

$$\hat{G}(\Omega_{k+iM}) = F \frac{Y_l(k+iM)}{U_h(k+iM)}, \quad \forall i \in \mathbb{Z}_{[0, F-1]}, (k+iM) \in \mathcal{S}, \quad (11)$$

given that the excitation signal is designed such that the output $Y_l(k)$ is only influenced by a single frequency of $U_h(k)$ according to (8). An example of a sparse multisine is shown in Example 1.

Example 1: An example of a sparse multisine, that achieves broadband excitation, is given by

$$U_h(k) \neq 0, \quad \forall k \in \mathcal{S}, \quad \mathcal{S} = \left\{ j + i(M+1) \mid \begin{array}{l} i \in \mathbb{Z}_{[0, F-1]}, \\ j \in \left\{ 0, F, 2F, \dots, \frac{1}{2}M \right\} \end{array} \right\}. \quad (12)$$

Essentially, the sparse multisines in Example 1 avoid interference of different frequency bands, and by appropriately selecting the inputs a system estimate \hat{G} is obtained at a sparse set of frequencies in each frequency band, including the bands beyond the Nyquist frequency.

The resulting estimate $\hat{G}(\Omega_k)$ is only obtained at the sparse set of excited bins $k \in \mathcal{S}$. By ranging i over multiple sets of experiments in $\{0, 1, \dots, F-1\}$, the system $\hat{G}(\Omega_k)$ can be uniquely recovered for the full frequency spectrum. As a result, F experiments are necessary to identify the system, which leads to a time-intensive procedure. In the next section, a time-efficient single-experiment identification approach is developed.

IV. IDENTIFICATION WITH FULL EXCITATION SPECTRUM

In this section, the approach is developed to identify a fast-sampled model of $G(\Omega_k)$ for all frequency bins $k \in \mathbb{Z}_{[0, N-1]}$, given slow-sampled outputs, therewith constituting contribution C1. This is realized by exciting the full frequency spectrum, where aliased contributions are disentangled by exploiting a smoothness condition on G and the transient.

In contrast to Section III, where for each frequency bin k the F unknowns in (7) were reduced to a single unknown as seen in (10), in this section the amount of equations are increased to F for each frequency bin k . First, the method is presented. Second, a covariance analysis is provided. Finally, the developed approach is summarized in a procedure.

A. Identification of Slow-Sampled Systems With Full Excitation Spectrum

The frequency response of the system $G(\Omega_k)$ and transient $T_G(\Omega_k)$ are assumed to be smooth, as is formalized in Assumption 1 and Assumption 2. The smoothness assumption enables disentangling aliased components, and consequently, the need for a sparse excitation signal in Section III is relaxed.

Assumption 1: The frequency response of the fast-sampled system $G(\Omega_k)$ can be approximated in a local window $r \in \mathbb{Z}_{[-n_w, n_w]}$, with $2n_w + 1$ the window size, as an R^{th} order polynomial as

$$G(\Omega_{k+r}) \approx G(\Omega_k) + \sum_{s=1}^R g_s(k)r^s, \quad (13)$$

Assumption 2: The summation of transients, seen in (6), is assumed to be smooth in the local window $r \in \mathbb{Z}_{[-n_w, n_w]}$, i.e.,

$$\frac{1}{F} \sum_{f=0}^{F-1} T_G(\Omega_{k+r+Mf}) \approx T(\Omega_k) + \sum_{s=1}^R t_s(k)r^s. \quad (14)$$

The assumption of a locally smooth system and transient is commonly imposed and at the basis of modern FRF identification, and is valid since $G(\Omega_k)$ and $T_G(\Omega_m)$ are functions with continuous derivatives up to any order [5], [16]. Hence, the assumption of a smooth summation of transients is equally reasonable, since the individual transient contributions are smooth. By substituting the polynomial models for $G(\Omega_k)$ in (13) and for the transient in (14), the slow-sampled output in (6) is rewritten with parameter vector Θ and data vector K for the local window r as

$$Y_l(k+r) = \Theta(k)K(k+r) + V_l(k+r). \quad (15)$$

The parameter vector $\Theta(k) \in \mathbb{C}^{1 \times (R+1)(F+1)}$ is given by

$$\Theta(k) = [\theta_G \ \theta_{g_1} \ \cdots \ \theta_{g_R} \ T(\Omega_k) \ t_1(k) \ \cdots \ t_R(k)], \quad (16)$$

with

$$\begin{aligned} \theta_G &= \frac{1}{F} [G(\Omega_k) \ G(\Omega_{k+M}) \ \cdots \ G(\Omega_{k+(F-1)M})], \\ \theta_{g_i} &= \frac{1}{F} [g_i(k) \ g_i(k+M) \ \cdots \ g_i(k+(F-1)M)], \end{aligned} \quad (17)$$

and data vector $K(k+r) \in \mathbb{C}^{(R+1)(F+1) \times 1}$ is given by

$$K(k+r) = \begin{bmatrix} K_1(r) \otimes \underline{U}(k+r) \\ K_1(r) \end{bmatrix}, \quad (18)$$

with input vector

$$\underline{U}(k+r) = \begin{bmatrix} U_h(k+r) \\ U_h(k+r+M) \\ \vdots \\ U_h(k+r+(F-1)M) \end{bmatrix}, \quad (19)$$

where $K_1(r) = [1 \ r \ \cdots \ r^R]^T$ and \otimes denotes the Kronecker product. Collecting the column vectors from (15) in matrices for the window $r \in \mathbb{Z}_{[-n_w, n_w]}$ gives

$$Y_{l, n_w} = \Theta(k)K_{n_w} + V_{n_w}, \quad (20)$$

where $Y_{l, n_w} \in \mathbb{C}^{1 \times 2n_w+1}$, $K_{n_w} \in \mathbb{C}^{(R+1)(F+1) \times 2n_w+1}$ and $V_{n_w} \in \mathbb{C}^{1 \times 2n_w+1}$ are constructed as

$$X_{n_w} = [X(k-n_w) \ X(k-n_w+1) \ \cdots \ X(k+n_w)]. \quad (21)$$

The fast-sampled system $G(\Omega_k)$ and transient $T(\Omega_k)$ are uniquely identifiable for all $k \in \mathbb{Z}_{[0, N-1]}$, in the presence of aliasing and with a full excitation spectrum, as in Theorem 1.

Theorem 1: Given a frequency bin k , if $M+1 > 2n_w+1 \geq (F+1)(R+1)$ and the input vector $\underline{U}(k+r)$ from (19) is designed such that K_{n_w} is of full row rank, an estimate of the parameter vector Θ in the least-squares sense of (20) is uniquely determined as

$$\hat{\Theta}(k) = Y_{l, n_w} K_{n_w}^H (K_{n_w} K_{n_w}^H)^{-1}, \quad (22)$$

and the fast-sampled model of system $G(\Omega_k)$ is obtained by

$$\hat{G}(\Omega_k) = F \hat{\Theta}(k) [1 \ 0_{1 \times ((F+1)(R+1)-1)}]^T. \quad (23)$$

Similarly, $\hat{T}(\Omega_k) = \frac{1}{F} \sum_{f=0}^{F-1} \hat{T}_G(\Omega_{k+Mf})$ from (14) can be obtained.

Proof: The matrix inverse $(K_{n_w} K_{n_w}^H)^{-1}$ uniquely exists if $(K_{n_w} K_{n_w}^H)$ has full rank, which is achieved if the rank of K_{n_w} is equal to the row rank of K_{n_w} and K_{n_w} is full row rank. ■

The interpretation of Theorem 1 is as follows. First, sufficient data $2n_w + 1$ should be available, such that (22) leads to a unique solution of the $(R+1)(F+1)$ parameters, hence $2n_w + 1 \geq (F+1)(R+1)$, which is satisfied by design of wide matrix K_{n_w} . In other words, by applying the smoothness assumption, the estimation of the $(R+1)(F+1)$ parameters $\hat{\Theta}$ in (22) utilizes $2n_w + 1$ outputs in $Y_l(k+r)$. This explains how the smoothness assumption allows to disentangle F aliased contributions at a frequency bin k . Additionally, no overlapping between windows $k+r+iM \ \forall i \in \mathbb{Z}_{[0, F-1]}$ is allowed, otherwise K_{n_w} is not full row rank, and hence, $M+1 > 2n_w+1$. Second, the system in (22) can be solved uniquely if K_{n_w} is full row rank. As a consequence, aliased and transient contributions can be disentangled if all inputs in the local window and at the aliased windows are sufficiently ‘rough’, that is formalized for a single local window in [18]. For Theorem 1, this means that the spectral difference $|U(k+r_1+iM) - U(k+r_2+iM)| \neq 0 \ \forall r_1, r_2 \in \mathbb{Z}_{[-n_w, n_w]}$, $\forall i \in \mathbb{Z}_{[0, F-1]}$. This condition is fulfilled by, e.g., random-phase multisines [5]. The developed framework is illustrated in Fig. 3.

Remark 1: Note that traditional LPM for single-rate LTI systems is recovered as a special case of the developed framework by setting $F = 1$.

Remark 2: The identified FRF by sparse multisines from Section III can be interpolated at the non-excited frequency bins $k \notin \mathcal{S}$, similar to [19], by seeing them as a special case of the framework in this section. The condition on $\underline{U}(k+r)$ in Theorem 1 is inherently satisfied by sparse excitation.

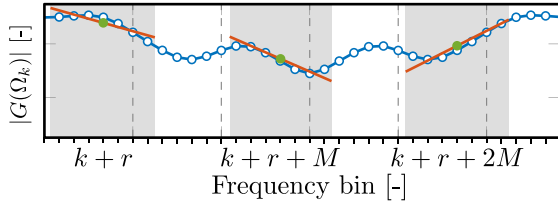


Fig. 3. Illustration of identification of slow-sampled system that disentangles aliased components by assuming local smoothness. True fast-sampled system $G(\Omega_k)$ (—○—), and the local first-order parametric estimates $\hat{G}(\Omega_{k+r+iM}) = \hat{G}(\Omega_{k+iM}) + g_1(k+iM)r \forall i \in \{0, 1, 2\}$ of the developed approach (—). The values $F = 3$, $R = 1$ and $n_w = 3$, when neglecting the transient, result in 6 unknowns, i.e., the system estimates $\hat{G}(\Omega_{k+iM})$ (●) and the polynomial coefficients $g_1(k+iM)$, that determine the slopes of (—). Since $n_w = 3$, there are in total $2n_w + 1 = 7$ equations, hence the system of equations in (22) can be solved for the 6 unknowns.

B. Variance Estimate of the FRF

The developed framework enables estimation of the variance of the identified FRF. The variance of \hat{G} , that is estimated using (22), is given by Theorem 2.

Theorem 2: The estimated variance of the FRF \hat{G} that is estimated using (23) is given by

$$\text{var}(\hat{G}(\Omega_k)) \approx F \overline{S^H S} \hat{C}_V(k), \quad (24)$$

that is an estimate of the true variance of the identified FRF

$$\text{var}(\hat{G}(\Omega_k)) = F \mathbb{E}\{\overline{S^H S}\} C_V(k) + FO_{intH} \left(\frac{n_w^0}{M} \right), \quad (25)$$

with C_V the variance of the noise and an estimate based on measurements \hat{C}_V , noise interpolation error O_{intH} [5], and

$$S = K_{n_w}^H (K_{n_w} K_{n_w}^H)^{-1} [1 \ 0]^T. \quad (26)$$

Proof: The proof extends [5, Appendix 7.E] to F frequency bands. In particular, by combining (20) and (22) into

$$\begin{aligned} (Y_{n_w} - \Theta K_{n_w}) S &= V_{n_w} S, \\ \underbrace{\hat{\Theta} [1 \ 0]^T}_{\frac{1}{F} \hat{G}} - \underbrace{\Theta [1 \ 0]^T}_{\frac{1}{F} G} &= V_{n_w} S, \\ \hat{G} &= G + F V_{n_w} S, \end{aligned} \quad (27)$$

the factor F appears in the difference between the true and estimated system G and \hat{G} . ■

The variance of the noise is equal to

$$C_V(k) = \text{var}(V_l(k)) = \mathbb{E}\{V_l(k) V_l^H(k)\}. \quad (28)$$

An estimate of the noise variance is calculated by taking an average over the local window, see [5, Appendix 7.B] for technical details, i.e.,

$$\hat{C}_V(k) = \frac{1}{2n_w + 1 - (R + 1)(F + 1)} \hat{V}_{n_w} \hat{V}_{n_w}^H, \quad (29)$$

with $\hat{V}_{n_w} = Y_{l,n_w} - \hat{\Theta}(k) K_{n_w}$.

C. Developed Procedure

The developed approach is summarized in Procedure 1, that links the main results in this letter.

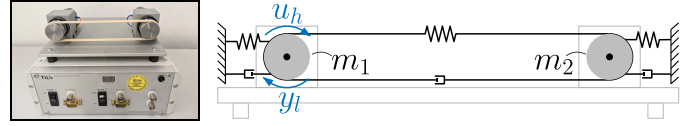


Fig. 4. Left: Picture of experimental setup used. Right: Schematic overview of experimental setup.

TABLE I
EXPERIMENTAL SETTINGS

Property	Variable	Value
Fast-sampling rate	$f_{s,h}$	120 Hz
Slow-sampling rate	$f_{s,l}$	30 Hz
Downsampling factor	F	4
Measurement time	T_m	120 s
Window size	n_w	150
Polynomial degree	R	2

V. VALIDATION

In this section, the developed method is validated on an experimental setup, leading to contribution C2.

A. Measurement Setup

The experimental setup is shown in Fig. 4. The setup consists of two rotating masses connected via a rubber band. The rotating masses are each actuated by a DC motor. The input u_h and output y_l are respectively the torque and rotation of the first mass. The second mass is virtually suspended to the fixed world by a feedback controller. The excitation signal for the developed approach that excites the full frequency spectrum is a random-phase multisine and has an root-mean-square value of $8.3 \cdot 10^{-3}$ Nm. For comparison purposes, the intuitive idea from Section III uses sparse multisines with a root-mean-square value of $9.6 \cdot 10^{-3}$ Nm and are designed as in Example 1. A photograph and a schematic overview of the test setup are seen in Fig. 4. The settings used during identification are shown in Table I.

B. Experimental Results

The fast-sampled system is identified using the developed approach from Section IV. For comparison purposes, the sparse multisine approach from Section III, a traditional approach and using the fast-sampled output y , that is not available for the other approaches, are used to identify the fast-sampled system. The results for the developed, sparse multisine and traditional approach are seen in Fig. 5, Fig. 6 and Fig. 7.

The following observations are made

- 1) From Fig. 5 and Fig. 6, it is observed that the developed approach and the sparse multisines are capable of identifying the dynamics above the Nyquist frequency of the sensor. The developed approach of Section IV that assumes smooth behavior in the frequency-domain has significantly lower variance and a factor F higher frequency resolution.
- 2) From Fig. 7, it is observed that exciting the system with the full frequency spectrum and performing FRF

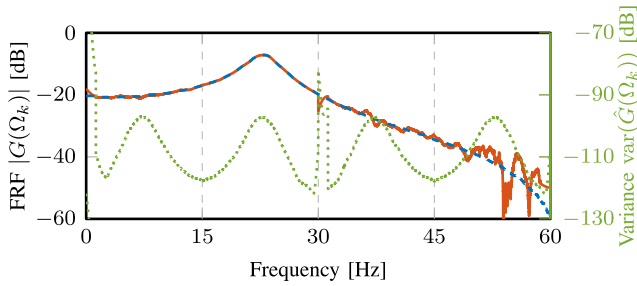


Fig. 5. Identified FRF $\hat{G}(\Omega_k)$ for excitation by random-phase multisines covering the full frequency spectrum from Section IV (—) with covariance estimate from (24) (···) (right axis). The identified FRF based on fast-sampled data is shown as (--) and multiples of the Nyquist frequency of the slow sensor as (-·-).

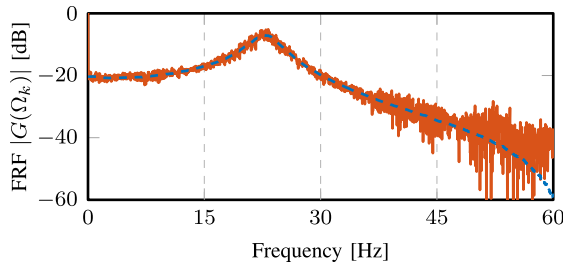


Fig. 6. Identified FRF $\hat{G}(\Omega_k)$ with sparse multisines from Section III in a single identification experiment (—). The identified FRF based on fast-sampled data is shown as (--) and multiples of the Nyquist frequency of the slow sensor as (-·-).

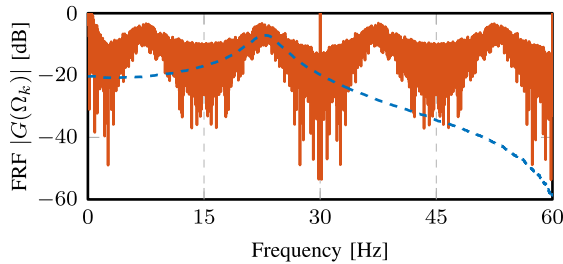


Fig. 7. Identified FRF $\hat{G}(\Omega_k)$ for excitation by full frequency spectrum random-phase multisines by performing $\hat{G}(\Omega_k) = Y_l(k)/U_h(k)$ using the same dataset as the full approach (—). The identified FRF based on fast-sampled data is shown as (--) and multiples of the Nyquist frequency of the slow sensor as (-·-).

identification by $\hat{G}(\Omega_k) = Y_l(k)/U_h(k)$ cannot accurately identify the fast-sampled system G , due to aliasing. Additionally, the estimated FRF is dominated by a periodic behavior, which is explained because the slow-sampled DFT $Y_l(k)$, that is M -periodic, is used for all frequencies and aliasing is not accounted for.

- 3) From Fig. 5, the variance of the developed approach that excites the full frequency spectrum repeats every f_l . For example, the increase of variance around 23 Hz repeats at 53 Hz. This is explained because the variance from (24) is determined with the estimated noise variance \hat{C}_v from (29), that uses the slow-sampled data Y_l , and hence, is periodic in f_l . Additionally, the mirroring effect that is observed, e.g., the increase of variance

at 23 Hz is mirrored to 7 and 37 Hz, is caused because the DFT of \hat{C}_v is symmetrical in $\frac{1}{2}f_l$.

VI. CONCLUSION

The results in this letter enable identifying FRFs of slow-sampled systems where aliasing occurs. The key step is assuming smooth behavior of the system FRF, which allows to appropriately disentangle aliased contributions when exciting the full frequency spectrum. Furthermore, covariance estimates of the FRF are provided. Finally, the framework is validated through experimental results. The dual case, where outputs are fast-sampled and inputs slow-sampled, is trivial by assuming appropriate interpolator behavior. The developed approach is a key enabler for closed-loop, multivariable and parametric system identification and control design for slow-sampled systems, such as vision-in-the-loop systems.

REFERENCES

- [1] C. E. Shannon, "Communication in the presence of noise," *Proc. IRE*, vol. 37, no. 1, pp. 10–21, 1949.
- [2] T. Oomen, M. van de Wal, and O. Bosgra, "Design framework for high-performance optimal sampled-data control with application to a wafer stage," *Int. J. Control*, vol. 80, no. 6, pp. 919–934, 2007.
- [3] R. M. Schmidt, G. Schitter, A. Rankers, and J. van Eijk, *The Design of High Performance Mechatronics*. Amsterdam, The Netherlands: Delft Univ. Press, 2020.
- [4] R. Pintelon, P. Guillaume, Y. Rolain, J. Schoukens, and H. van Hamme, "Parametric identification of transfer functions in the frequency domain—a survey," *Trans. Autom. Control*, vol. 39, no. 11, pp. 2245–2260, 1994.
- [5] R. Pintelon and J. Schoukens, *System Identification: A Frequency Domain Approach*. Hoboken, NJ, USA: Wiley, 2012.
- [6] T. Oomen, "Advanced motion control for precision mechatronics: Control, identification, and learning of complex systems," *IEEE J. Ind. Appl.*, vol. 7, no. 2, pp. 127–140, 2018.
- [7] S. Skogestad and I. Postlethwaite, *Multivariable Feedback Control—Analysis and Design*. Hoboken, NJ, USA: Wiley, 2005.
- [8] K. J. Åström and B. Wittenmark, *Computer-Controlled Systems: Theory and Design*. Englewood Cliffs, NJ, USA: Dover Publ., 2011.
- [9] H. Unbehauen and G. P. Rao, "Continuous-time approaches to system identification—A survey," *Automatica*, vol. 26, no. 1, pp. 23–35, 1990.
- [10] L. Ljung, "Experiments with identification of continuous time models," *IFAC Proc. Vol.*, vol. 42, no. 10, pp. 1175–1180, 2009.
- [11] F. Ding and T. Chen, "Identification of dual-rate systems based on finite impulse response models," *Int. J. Adapt. Control Signal Process.*, vol. 18, no. 7, pp. 589–598, 2004.
- [12] Y. Zhu, H. Telkamp, J. Wang, and Q. Fu, "System identification using slow and irregular output samples," *J. Process Control*, vol. 19, no. 1, pp. 58–67, 2009.
- [13] D. Li, S. L. Shah, and T. Chen, "Identification of fast-rate models from multirate data," *Int. J. Control*, vol. 74, no. 7, pp. 680–689, 2001.
- [14] M. van Haren, L. Blanken, and T. Oomen, "Frequency domain identification of multirate systems: A lifted local polynomial modeling approach," in *Proc. Conf. Decis. Control*, 2022, pp. 2795–2800.
- [15] J. Ding, F. Ding, X. P. Liu, and G. Liu, "Hierarchical least squares identification for linear SISO systems with dual-rate sampled-data," *Trans. Autom. Control*, vol. 56, no. 11, pp. 2677–2683, 2011.
- [16] T. McKelvey and G. Guérin, "Non-parametric frequency response estimation using a local rational model," *IFAC Proc. Vol.*, vol. 45, no. 16, pp. 49–54, 2012.
- [17] P. Vaidyanathan, *Multirate Systems and Filter Banks*. Englewood Cliffs, NJ, USA: Prentice-Hall, 1993.
- [18] J. Schoukens, G. Vandersteen, K. Barbé, and R. Pintelon, "Nonparametric preprocessing in system identification: A powerful tool," *Eur. J. Control*, vol. 15, nos. 3–4, pp. 260–274, 2009.
- [19] E. Geerardyn and T. Oomen, "A local rational model approach for \mathcal{H}_∞ norm estimation: With application to an active vibration isolation system," *Control Eng. Pract.*, vol. 68, pp. 63–70, 2017.